Trajectory Optimization of Autonomous Agents with Spatio-Temporal Constraints

Xiangyu Meng, and Christos G. Cassandras, Fellow, IEEE

Abstract—This paper addresses the problem of optimally controlling trajectories of autonomous mobile agents (e.g., robots) so as to jointly minimize travel time and energy consumption in the presence of multiple spatiotemporal constraints on these trajectories. In addition to state and input constraints, we impose spatial equality and temporal inequality constraints viewed as interior-point constraints. We address this problem by first identifying the structure of the optimal agent controllable acceleration profile and showing that it is characterized by several parameters subsequently used for trajectory design optimization. Therefore, the infinite dimensional optimal control problem is transformed into a finite dimensional parametric optimization problem. The proposed algorithm is applied to the eco-driving problem of autonomous vehicles approaching multiple signalized intersections. We include simulation results to show quantitatively the advantages of the proposed solution.

Index Terms—Autonomous agents, intelligent vehicles, optimal control, spatio-temporal constraints, trajectory optimization

I. Introduction

THE operation of autonomous mobile agents, such as autonomous vehicles and unmanned aerial vehicles, requires an agent to travel on a planned reference trajectory. Applications include coverage control [1]–[3], intersection control of connected automated vehicles [4], [5], data harvesting [6], and persistent monitoring [7]–[10]. Often, these tasks are dictated under a requirement for both time and energy efficiency. Therefore, it is essential to develop realtime optimal control algorithms to enable such tasks.

In this paper, we focus on a class of problems in which a mobile agent (e.g., robot) follows a predetermined reference trajectory which includes a series of "gateways" whose state switches over time between open and closed, thus defining both spatial and temporal constraints. An additional requirement is to finish this task in a way which is both time and energy efficient. Such problems are usually solved by using temporal logic and formal methods [11], [12]. Here, we aim to tackle this problem by using calculus of variations

This work was supported in part by NSF under grants ECCS-1509084, DMS-1664644, CNS-1645681, by AFOSR under grant FA9550-19-1-0158, by ARPA-Es NEXTCAR program under grant DE-AR0000796 and by the MathWorks.

X. Meng is with the Division of Electrical and Computer Engineering, Louisiana State University, Baton Rouge, LA 70803 USA (e-mail: xmeng5@lsu.edu).

C. G. Cassandras is with the Division of Systems Engineering and Center for Information and Systems Engineering, Boston University, Brookline, MA 02446 USA (e-mail: cgc@bu.edu).

methods within the optimal control framework [22]. There are several aspects of this problem that make it challenging. The major one is the switching of the gateway states which makes crossing the gateway impossible for a period of time. This can be modeled via interior point constraints. The interior point constraints include specifically spatial equality constraints which relate to the location of gateways and temporal inequality constraints which characterize the gateway open time. Note that the unavailability of gateway access creates discontinuities in the feasible space of the gateway crossing time. These discontinuities lead to non-convex optimization problems in which the global optimal solution is not generally guaranteed. However, it follows from the theoretical analysis that the optimal controllable acceleration profile can be parameterized by a piece-wise linear function of time. Due to the speed and acceleration constraints, we show that there is only a limited number of cases for each gateway crossing time, which greatly reduces the feasible range of each such variable. After determining each gateway crossing interval, the dynamic trajectory optimization problem is transformed into an equivalent much simpler static parameter optimization problem.

One particular application of the above problem is the ecodriving of a single autonomous vehicle or the leading autonomous vehicle of a platoon approaching multiple signalized intersections in the free flow mode. In this case, an intersection corresponds to a "gateway" and the traffic light signaling mechanism is the switching controller that provides access to it. The term "ECO-AND" (short for "Economical Arrival and Departure") is coined in the literature to refer to this problem [13]. The solution of the ECO-AND problem is made possible by vehicle-to-infrastructure (V2I) communication, which enables a vehicle to automatically receive signals from upcoming traffic lights before they appear in its visual range. Along these lines, the problem of avoiding red traffic lights is investigated in [4], [14]–[19]. Most existing work solves the eco-driving problem with traffic light constraints numerically, invoking methods such as using dynamic programming [4], and model predictive control [14]. Such numerical approaches may have the advantage of incorporating complex models. However, to enable the real-time use of such eco-driving methods, it is desirable to have an on-line analytical solution. If one is available, then whenever a vehicle is rerouted, a solution can be calculated with new initial conditions. In addition, an analytical solution provides a reference trajectory and a theoretical performance bound. The eco-driving problem for a single isolated signalized intersection was addressed in [20].

The approach proposed here considers multiple intersections as a whole and includes the single intersection scenario as a special case. Moreover, additional constraints, such as driving comfort, or constrained turning speed, can be added to make the solution more practical. Our analysis offers a real-time analytical solution to eco-driving of autonomous vehicles crossing multiple signalized intersections without stopping. We illustrate the effectiveness of the proposed optimal parametric approach through several simulation examples and show that it yields better results compared with our previous eco-driving approach [20] applied to each intersection individually.

The key contributions of this paper are as follows: (i) We characterize the form of the optimal acceleration profile for a class of trajectory optimization problems subject to spatio-temporal constraints. (ii) The proposed parametrization approach is applied to the eco-driving problem of autonomous vehicles approaching multiple signalized intersections. (iii) The eco-driving problem is equivalently transformed into a solvable parameter optimization problem which enables a real-time online implementation.

The rest of the paper is organized as follows. In Section II, we formulate the autonomous mobile agent trajectory optimization problem including spatio-temporal constraints. Section III gives an in-depth analysis of the form of the optimal acceleration solution, and discusses its parametrization. Section IV presents the extension to N gateways and specialization to 1 gateway. Section V uses the proposed framework to design the optimal acceleration profile for autonomous vehicles approaching multiple signalized intersections, followed by simulation results in Section VI. Section VII offers conclusive statements derived from the theoretical analysis and simulation results.

II. PROBLEM FORMULATION

An agent travels on a pre-calculated route from origin to destination. There are N gateways (as defined in the Introduction) along the path. The distance between the agent's initial location to the first gateway is l_1 , and the distance between gateway i and gateway i-1 is l_i as shown in Fig. 1. For each gateway i, there are alternating open and closed intervals, which are denoted as T_i^o (green lines in Fig. 1) and T_i^c (red lines in Fig. 1), respectively. When an agent arrives at gateway i at $t \in T_i^o$, it can go through the gateway right away. However, if the agent arrives at gateway i at $t \in T_i^c$, it has to wait until the gateway is open. Therefore, its gateway crossing time belongs to the set $\{\hat{t} \geq t | \hat{t} \in T_i^o\}$. Note that the gateway open and closed intervals are nonuniform, and we assume that the information is available to the agent.

The autonomous mobile agent dynamics are modeled by a double integrator

$$\dot{x}(t) = v(t), \qquad \dot{v}(t) = u(t), \tag{1}$$

where $x\left(t\right)$ is the travel distance of the mobile agent relative to some origin, $v\left(t\right)$ the velocity, and $u\left(t\right)$ the acceleration/deceleration. At t_0 , the initial travel distance and velocity are given by $x\left(t_0\right)=x_0$ and $v\left(t_0\right)=v_0$, respectively. The agent has the minimum and maximum speed constraints

$$0 \le v_{\min} \le v(t) \le v_{\max},\tag{2}$$

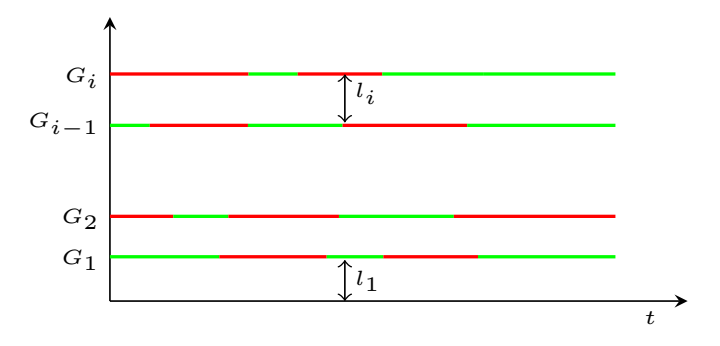


Fig. 1. A sample of gateway locations and open/closed time

where $v_{\rm min}$ and $v_{\rm max}$ are the minimum and maximum permissible speed of the mobile agent, respectively. The physical constraints on acceleration and deceleration are given by

$$u_{\min} \le u(t) \le u_{\max},$$
 (3)

where $u_{\min} < 0$ and $u_{\max} > 0$ denote the maximum deceleration and acceleration, respectively.

Let $\{t_i\}_{i=1}^N$ be a sequence of times when an agent crosses the gateways with $t_{i+1} > t_i$. This also implies that $x(t_i) = \sum_{j=1}^i l_j$. Since t_i is the gateway crossing time, it must be within the gateway open interval, that is, $t_i \in T_i^o$.

Our objective is to optimize the trajectory of the agent going through all gateways in terms of both travel time, which is defined by the time when the last gateway is crossed, and energy consumption. The objective function is

$$J = \rho_t (t_N - t_0) + \rho_u \int_{t_0}^{t_N} u^2(t) dt,$$
 (4)

where ρ_t and ρ_u are weight parameters to normalize the two terms in (4) for the purpose of a well-defined optimization problem, and t_N is the time when the agent passes through the last gateway. Here $J^t=t_N-t_0$ is the trip time, and we define

$$J^{u} = \int_{t_{0}}^{t_{N}} u^{2}(t) dt$$
 (5)

as a measure of the energy cost.

Therefore, the problem formulation of the trajectory optimization problem with spatio-temporal constraints (TOSTC) is given below:

Problem 1: TOSTC Problem

$$\min_{u(t)} \rho_t \left(t_N - t_0 \right) + \rho_u \int_{t_0}^{t_N} u^2 \left(t \right) dt$$

subject to (1) and

$$x(t_i) = \sum_{j=1}^{i} l_j, \ i = 1, \dots, N$$
 (6)

$$v_{\min} \le v\left(t\right) \le v_{\max} \tag{7}$$

$$u_{\min} \le u(t) \le u_{\max} \tag{8}$$

$$t_i \in T_i^o, \ i = 1, \dots, N.$$
 (9)

Due to the discontinuity of the gateway open interval T_i^o , gradient-based algorithms are not applicable to this problem. To make the problem solvable, a pruning algorithm may be used firstly to identify all possible paths by taking advantage of the velocity and acceleration constraints, and traffic signal

phase and timing information [18]. After all feasible gateway crossing time intervals have been found, the solutions in Section III to the optimization problems can determine the optimal gateway crossing time with a known gateway crossing time interval. Lastly, the performance of all possible paths is compared to select the optimal one. Details are omitted and we instead make the assumption that the optimal gateway crossing time t_i is unknown but it belongs to a subset of the gateway open set T_i^o , that is, $t_i \in [\underline{t}_i, \overline{t}_i] \subseteq T_i^o$ with known \underline{t}_i and \overline{t}_i .

III. MAIN RESULTS

Before proceeding further, let us introduce a lemma, which will be used subsequently.

Lemma 1: Consider the agent's dynamics (1) with initial conditions x_0 and v_0 . If the acceleration or deceleration profile of the agent has the form u(t) = at + b during the time interval $[t_0, t_1]$, where a and b are two constants, then

$$v(t_1) = v_0 + b(t_1 - t_0) + \frac{a}{2}(t_1^2 - t_0^2),$$

$$x(t_1) = x_0 + v_0(t_1 - t_0) + \frac{1}{2}b(t_1 - t_0)^2 + \frac{a}{6}(t_1^3 + 2t_0^3 - 3t_0^2t_1),$$

$$J^u = \frac{a^2}{3}(t_1^3 - t_0^3) + ab(t_1^2 - t_0^2) + b^2(t_1 - t_0),$$

where J^u is defined in Section II.

The proof is straightforward by integrating the kinematic model in (1) and by using the definition of J^u in (5).

In order not to overshadow the main ideas in our analysis, we consider the case of two gateways initially. Then, we will show how the proposed method is applicable to multiple gateways.

A. Optimal Control Analysis

The main challenge stems from the interior-point constraints (6) and (9), which are spatial equality constraints and temporal inequality constraints, respectively. Other constraints, such as state, acceleration/deceleration, and terminal constraints, can be studied using the direct adjoining approach [21]. The following theorem shows the optimal acceleration profile when the interior-point constraints are imposed.

Theorem 1: The optimal acceleration $u^*(t)$ of Problem 1 has the form $u^*(t) = a(t)t + b(t)$, where a(t) and b(t) are piece-wise constant functions of t.

Proof: The interior-point constraints are dealt with by using the calculus of variations methodology borrowed from [22] with certain modifications. The Hamiltonian $H(v,u,\lambda)$ and Lagrangian $L(v,u,\lambda,\mu,\eta)$ are defined as

$$H(v, u, \lambda) = \rho_t + \rho_u u^2(t) + \lambda_1(t) v(t) + \lambda_2(t) u(t)$$

and

$$\begin{split} L\left(v, u, \lambda, \mu, \eta\right) &= H\left(v, u, \lambda\right) \\ &+ \eta_{1}\left(t\right) \left[v_{\min} - v\left(t\right)\right] + \eta_{2}\left(t\right) \left[v\left(t\right) - v_{\max}\right] \\ &+ \mu_{1}\left(t\right) \left[u_{\min} - u\left(t\right)\right] + \mu_{2}\left(t\right) \left[u\left(t\right) - u_{\max}\right], \end{split}$$

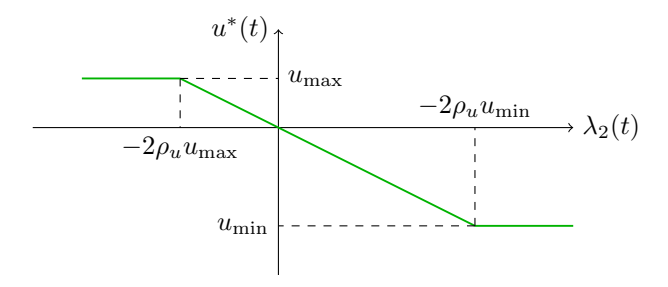


Fig. 2. Optimality relationship between $u^*(t)$ and $\lambda_2(t)$

respectively, where $\lambda\left(t\right) = \left[\lambda_{1}\left(t\right) \ \lambda_{2}\left(t\right)\right]^{T}, \ \mu\left(t\right) = \left[\mu_{1}\left(t\right) \ \mu_{2}\left(t\right)\right]^{T}, \ \eta\left(t\right) = \left[\eta_{1}\left(t\right) \ \eta_{2}\left(t\right)\right]^{T}, \text{ and}$

$$\eta_1(t) \ge 0, \ \eta_2(t) \ge 0,$$
(10)

$$\eta_1(t) \left[v_{\min} - v(t) \right] + \eta_2(t) \left[v(t) - v_{\max} \right] = 0,$$
 (11)

$$\mu_1(t) \ge 0, \ \mu_2(t) \ge 0,$$
 (12)

$$\mu_1(t) [u_{\min} - u(t)] + \mu_2(t) [u(t) - u_{\max}] = 0.$$
 (13)

According to Pontryagin's minimum principle, the optimal control $u^{*}\left(t\right)$ must satisfy

$$u^{*}\left(t\right) = \arg\min_{u_{\min} \leq u(t) \leq u_{\max}} H\left(v^{*}\left(t\right), u\left(t\right), \lambda^{*}\left(t\right)\right), \quad (14)$$

where * denotes optimal quantities. The Hamiltonian H can be viewed as a quadratic function in u. The minimum of H depends on the relationship between $-\frac{\lambda_2}{2\rho_u}$ and the range $[u_{\min},u_{\max}]$. When $-\frac{\lambda_2}{2\rho_u}\in[u_{\min},u_{\max}]$, H attains its minimum at $u=-\frac{\lambda_2}{2\rho_u}$. If $-\frac{\lambda_2}{2\rho_u}\geq u_{\max}$, then H attains its minimum at u_{\max} ; if $-\frac{\lambda_2}{2\rho_u}\leq u_{\min}$, then H attains its minimum at u_{\min} . Therefore, we can express $u^*(t)$ in terms of the co-state $\lambda(t)$, resulting in

$$u^*(t) = \begin{cases} u_{\text{max}} & \text{when } -\frac{\lambda_2(t)}{2\rho_u} \ge u_{\text{max}} \\ -\frac{\lambda_2(t)}{2\rho_u} & \text{when } u_{\text{min}} \le -\frac{\lambda_2(t)}{2\rho_u} \le u_{\text{max}} \\ u_{\text{min}} & \text{when } -\frac{\lambda_2(t)}{2\rho_u} \le u_{\text{min}} \end{cases}$$
(15)

Based on the optimality condition (15), the relationship between $\lambda_2(t)$ and $u^*(t)$ can be visualized as shown in Fig. 2. For simplicity, we write L(t), H(t), $\Phi(t)$ and N(t) without the arguments of states, co-states, and multipliers in the rest of the paper. Adjoin the system dynamics (1) to L(t) with multiplier function $\lambda(t)$:

$$\Phi(t) = N(t_1, t_2) + \int_{t_0}^{t_2} [L(t) - \lambda_1(t) \dot{x}(t) - \lambda_2(t) \dot{v}(t)] dt,$$

where t_1 is the first gateway crossing time, and

$$\begin{split} N\left(t_{1},t_{2}\right) &= \nu\left(x\left(t_{2}\right) - l_{1} - l_{2}\right) + \pi\left(x\left(t_{1}\right) - l_{1}\right) \\ &+ \xi_{1}\left(\underline{t}_{1} - t_{1}\right) + \xi_{2}\left(t_{1} - \bar{t}_{1}\right) + \xi_{3}\left(\underline{t}_{2} - t_{2}\right) + \xi_{4}\left(t_{2} - \bar{t}_{2}\right), \\ \xi_{1} &\geq 0, \quad \xi_{2} \geq 0, \quad \xi_{3} \geq 0, \quad \xi_{4} \geq 0, \\ \xi_{1}\left(\underline{t}_{1} - t_{1}\right) + \xi_{2}\left(t_{1} - \bar{t}_{1}\right) = 0, \xi_{3}\left(\underline{t}_{2} - t_{2}\right) + \xi_{4}\left(t_{2} - \bar{t}_{2}\right) = 0. \end{split}$$

The differential of Φ , taking into account differential changes in t_1 and t_2 , is

$$\begin{split} d\Phi\left(t\right) = &dN\left(t_{1},t_{2}\right) \\ &+ d\int_{t_{0}}^{t_{2}} \left[L\left(t\right) - \lambda_{1}\left(t\right)\dot{x}\left(t\right) - \lambda_{2}\left(t\right)\dot{v}\left(t\right)\right]dt. \end{split}$$

Split the integral into two parts:

$$\begin{split} d\Phi\left(t\right) &= \nu dx \left(t_{2}\right) + \left(\xi_{4} - \xi_{3}\right) dt_{2} + \left(\xi_{2} - \xi_{1}\right) dt_{1} + \pi dx \left(t_{1}\right) \\ &+ \left[L\left(t\right) - \lambda_{1}\left(t\right) \dot{x}\left(t\right) - \lambda_{2}\left(t\right) \dot{v}\left(t\right)\right] \big|_{t=t_{1}^{-}} dt_{1} \\ &- \left[L\left(t\right) - \lambda_{1}\left(t\right) \dot{x}\left(t\right) - \lambda_{2}\left(t\right) \dot{v}\left(t\right)\right] \big|_{t=t_{1}^{+}} dt_{1} \\ &- \lambda_{1}\left(t\right) \delta x\left(t\right) \big|_{t_{0}^{-}}^{t_{1}^{-}} - \lambda_{1}\left(t\right) \delta x\left(t\right) \big|_{t_{1}^{+}}^{t_{2}} \\ &- \lambda_{2}\left(t\right) \delta v\left(t\right) \big|_{t_{0}^{-}}^{t_{1}^{-}} - \lambda_{2}\left(t\right) \delta v\left(t\right) \big|_{t_{1}^{+}}^{t_{2}} \\ &+ \int_{t_{0}}^{t_{2}} \left[\dot{\lambda}_{2}\left(t\right) + \frac{\partial L\left(t\right)}{\partial v\left(t\right)}\right] \delta v\left(t\right) dt \\ &+ \int_{t_{0}}^{t_{2}} \left\{ \left[\dot{\lambda}_{1}\left(t\right) + \frac{\partial L\left(t\right)}{\partial x\left(t\right)}\right] \delta x\left(t\right) + \frac{\partial L\left(t\right)}{\partial u\left(t\right)} \delta u\left(t\right) \right\} dt, \end{split}$$

where we let t_1^- signify just before t_1 and t_1^+ signify just after t_1 . Next, we choose the functions $\lambda_1(t)$ and $\lambda_2(t)$ to make the coefficients of $\delta x(t)$ and $\delta v(t)$ vanish. We now make use of the relationships

$$dx\left(t_{1}\right) = \begin{cases} \delta x\left(t_{1}^{-}\right) + \dot{x}\left(t_{1}^{-}\right) dt_{1}, \\ \delta x\left(t_{1}^{+}\right) + \dot{x}\left(t_{1}^{+}\right) dt_{1}, \end{cases}$$

and similar expressions can be derived for $dx(t_2)$ and $dv(t_1)$. Using the above relationships to eliminate $\delta x(t_1^-)$ and $\delta x(t_1^+)$, and regrouping terms, yields

$$d\Phi(t) = [\nu - \lambda_{1}(t)] \delta x(t) |_{t=t_{2}} - \lambda_{2}(t) \delta v(t) |_{t=t_{2}}$$

$$+ \lambda_{1}(t) \delta x(t) |_{t=t_{0}} + \lambda_{2}(t) \delta v(t) |_{t=t_{0}}$$

$$+ [L(t_{1}^{-}) - L(t_{1}^{+}) + \xi_{2} - \xi_{1}] dt_{1}$$

$$+ [\lambda_{1}(t_{1}^{+}) - \lambda_{1}(t_{1}^{-}) + \pi] dx(t_{1})$$

$$+ [\lambda_{2}(t_{1}^{+}) - \lambda_{2}(t_{1}^{-})] dv(t_{1}) + (\xi_{4} - \xi_{3}) dt_{2}$$

$$+ \int_{t_{0}}^{t_{2}} \frac{\partial L(t)}{\partial u(t)} \delta u(t) dt.$$
(16)

Let us assume that $v(t_1) \neq v_{\max}$ and $v(t_1) \neq v_{\min}$. If $v(t_1) = v_{\max}$ or $v(t_1) = v_{\min}$, the problem can be decoupled at time t_1 as discussed in Remark 1. Since we have no constraints on v(t) at $t = t_1$, it follows that $\lambda_2\left(t_1^+\right) = \lambda_2\left(t_1^-\right)$, that is to say, there are no discontinuities in $\lambda_2\left(t\right)$ at $t = t_1$. Therefore, $u^*\left(t\right)$ is continuous everywhere based on (14) and Theorem 1 in [20]. To make the term $\lambda_2(t_2)\delta v(t_2)$ in (16) vanish, we must have $\lambda_2(t_2) = 0$ since there are no constraints on v(t) at $t = t_2$. From the optimality condition (15), we have $u^*(t_2^*) = 0$.

For the co-state $\lambda_1(t)$, we have $\dot{\lambda}_1(t) = -\frac{\partial L(t)}{\partial x} = 0$. However, since $dx(t_1) = 0$, $\lambda_1(t)$ may or may not have jumps at $t = t_1$. Therefore, $\lambda_1(t)$ can be written as

$$\lambda_{1}(t) = \begin{cases} \lambda_{1}^{-} & \text{for } t_{0} \leq t \leq t_{1}^{-}, \\ \lambda_{1}^{+} & \text{for } t_{1}^{+} \leq t \leq t_{2}. \end{cases}$$
 (17)

For the co-state $\lambda_2(t)$, we have

$$\dot{\lambda}_{2}\left(t\right) = -\frac{\partial L\left(t\right)}{\partial v} = -\lambda_{1}\left(t\right) + \eta_{1}\left(t\right) - \eta_{2}\left(t\right). \tag{18}$$

Depending on the value of v(t), we have different cases:

Case I: $v_{\min} < v(t) < v_{\max}$. In this case, $\eta_1(t) = \eta_2(t) = 0$. Therefore, $\lambda_2(t)$ linearly increases or decreases according to (17) and (18), and so does $u^*(t)$ based on (15).

Case II: $v\left(\tau\right)=v_{\min}$, where τ is the time when $v(t)=v_{\min}$. In this case, we have $u^*\left(t\right)\geq 0$ over some interval $[\tau,\tau+\alpha]$, where α is a positive scalar. When $u^*\left(t\right)=0$ over the interval $[\tau,\tau+\alpha]$, we must have $\lambda_2(t)=\dot{\lambda}_2(t)=0$, that is, $\eta_1\left(t\right)=\lambda_1\left(t\right)$ from (18) and the fact that $\eta_2(t)=0$ based on (11). When $u^*\left(\tau^+\right)>0$, $v\left(\tau^+\right)>v_{\min}$. Then, it becomes Case I.

Case III: $v\left(\tau\right)=v_{\mathrm{max}}$, where τ is the time when $v(t)=v_{\mathrm{max}}$. In this case, we have $u^*\left(t\right)\leq 0$ over some interval $\left[\tau,\tau+\alpha\right]$. When $u^*\left(t\right)=0$ over the interval $\left[\tau,\tau+\alpha\right]$, we have $\lambda_2(t)=\dot{\lambda}_2(t)=0$, that is, $\eta_2\left(t\right)+\lambda_1\left(t\right)=0$ from (18) and the fact that $\eta_1(t)=0$ based on (11). When $u^*\left(\tau^+\right)<0$, $v\left(\tau^+\right)< v_{\mathrm{max}}$. Then, it becomes Case I.

Regardless of which of these three cases applies, $\lambda_2(t)$ always has a linear form based on (18). Therefore, the optimal control $u^*(t)$ always has a linear form.

Remark 1: Assume that at t_1 all the state and acceleration/deceleration constraints are relaxed. Then L(t) is the same as H(t). To cause the coefficient of dt_1 in (16) to vanish, the condition $L(t_1^-) - L(t_1^+) + \xi_2 - \xi_1 = 0$ has to be satisfied. If $\underline{t}_1 < t_1 < \overline{t}_1$, then $\xi_1 = \xi_2 = 0$. Therefore, there are no jumps in L(t) and H(t) at t_1 . In other words, the co-state λ_1 has no jumps in this case. However, when $t_1 = \underline{t}_1$ or $t_1 = \bar{t}_1$, there may be jumps in L(t) and H(t) at t_1 . Then λ_1 switches from one value to another as shown in (17). When $v(t_1) = v_{\text{max}}$ or $v(t_1) = v_{\text{min}}$, the problem can be decoupled at time t_1 . Then, we have $dv(t_1) = 0$, and $\lambda_2(t)$ may have jumps at t_1 , and so may u(t) at t_1 . A jump in u(t) leads to a jerk effect, which is the rate of change of acceleration; that is, $\dot{u}(t)$. When the application of the proposed approach is to control autonomous vehicles which will be shown in Section V, we enforce no jumps in u(t) at t_1 so as to ensure passenger riding comfort.

Based on Theorem 1, specifically (15), we know that the optimal acceleration profile has the form $u^*(t) = a(t) t + b(t)$, where a(t) and b(t) are piece-wise constant functions. For example, we have a(t) = 0, $b(t) = u_{\text{max}}$ for $u^*(t) =$ u_{max} , and a(t) = 0, $b(t) = u_{\text{min}}$ for $u^*(t) = u_{\text{min}}$. For the case that u(t) = 0, we could set a(t) = b(t) = 0. When a(t) = a and b(t) = b are constants, the profile is either linear acceleration (a > 0) or deceleration (a < 0). In addition, there are only a few time instants when a(t)and b(t) switch from a constant to another. Such instants include the time when the maximum acceleration starts to decrease, the maximum deceleration starts to increase, the vehicle reaches the maximum or the minimum allowed speed limits, or the agent is located at the first gateway. Therefore, we can parameterize the optimal acceleration profile by a sequence of linear functions of time.

B. Parametric Optimization

According to Theorem 1, we are able to parameterize the optimal control in terms of piece-wise linear acceleration/deceleration. Then, we can transform the dynamic optimization problem into a static optimization problem by finding the optimal values of a few parameters. Based on the analysis of the last section, the optimal acceleration profile can be

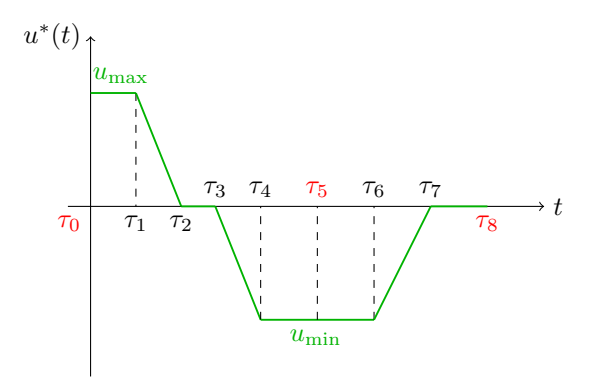


Fig. 3. A sample optimal acceleration profile for two intersections, where the time instants in red signify the gateway crossing time

parameterized by a sequence of linear functions of time, such as the one shown in Fig. 3, where $\tau_0=t_0$ is the initial time, $\tau_5=t_1$ is the first gateway crossing time, and $\tau_8=t_2$ is the second gateway crossing time. The optimal acceleration profile at most has six switches based on the optimality condition (15) and the following facts:

- u* (t₂) = 0, which can be seen from the proof of Theorem 1.
- Whenever $v(t) = v_{\min}$ or v_{\max} , $u^*(t) = 0$.
- $u^*(t)$ is continuous without jumps.
- Only at t_1 , $\dot{\lambda}_2(t)$ may change sign from nonnegative to nonpositive and vice versa (i.e., from nonpositive to nonnegative) according to (18).

The above facts are discussed as follows. To make the term $\lambda_2(t_2)\delta v(t_2)$ in (16) vanish, we must have $\lambda_2(t_2)=0$ since there are no constraints on v(t) at $t=t_2$. From the optimality condition (15), we have $u^*(t_2)=0$. The second observation above corresponds to the intervals $[\tau_2,\tau_3]$ and $[\tau_7,\tau_8]$ in Fig. 3, in which $v(t)=v_{\max}$ for $t\in[\tau_2,\tau_3]$ and $v(t)=v_{\min}$ for $t\in[\tau_7,\tau_8]$, respectively. The fourth observation above can be visualized in Fig. 3 as well. Before τ_5 , the acceleration decreases monotonically; and after τ_5 it increases monotonically.

Before t_1 , there are at most 4 switches of $u^*(t)$ assuming that $\lambda_2(t)$ starts from either the far left or the far right as seen from Fig. 2. At time t_1 , $\lambda_2(t)$ may change its direction. After t_1 , there are at most 2 switches of $u^*(t)$. The last switch may be due to $\lambda_2(t) = 0$ and $\lambda_2(t) = 0$ since the optimality condition indicates that $u^*(t_2) = 0$. Figure 3 corresponds to the following case. Assume that $\lambda_2^*(\tau_0) < -2\rho_u u_{\text{max}}$. Based on (15), $u^*(\tau_0) = u_{\text{max}}$. During the interval $t \in (\tau_0, \tau_1)$, $\dot{\lambda}_2^*(t)>0$ and $\lambda_2^*(t)<-2
ho_u u_{\max}$, then $u^*(t)=u_{\max}$. At time τ_1 , $\lambda_2^*(\tau_1) = -2\rho_u u_{\text{max}}$. During the interval $t \in (\tau_1, \tau_2)$, $\lambda_2^*(t) > 0$ and $u^*(t)$ starts to decrease based on Fig. 2 until τ_2 when $u^*(\tau_2) = 0$ and $v^*(\tau_2) = v_{\text{max}}$. During the interval $t \in (\tau_2, \tau_3)$, it is possible that $\eta_2(t) = -\lambda_1^-$ and $\dot{\lambda}_2^*(t) = 0$. After τ_3 , the agent starts deceleration until τ_4 when $\lambda_2^*(\tau_4) =$ $-2\rho_u u_{\min}$. Then $u^*(t) = u_{\min}$ for $t \in [\tau_4, \tau_5]$. After the first gatewat at τ_5 , $\dot{\lambda}_2^*(t) < 0$. When the velocity $v^*(\tau_7) = v_{\min}$, this may hold until the second gateway at time τ_8 . A similar optimal acceleration profile to the one in Fig. 3 can be drawn when it starts with the maximum deceleration.

Even though there are seven linear functions in Fig. 3, eight linear functions are needed to parameterize the acceleration profile, as explained next. Over the interval $[\tau_4, \tau_6]$ in Fig. 3, there is only one linear function. In order to guarantee that the gateway crossing time is within the open interval, the constraint (26) is added below, where τ_5 is denoted as t_1 . Therefore, two linear functions are used to parameterize the optimal acceleration profile. We can thus parameterize the optimal acceleration profile as follows:

$$u^*(t) = a_i t + b_i \text{ for } t \in [\tau_{i-1}, \tau_i]$$
 (19)

for i = 1, 2, ..., 8, where $\tau_0 = t_0$, $\tau_5 = t_1$, and $\tau_8 = t_2$.

Remark 2: The optimal acceleration profile is over parameterized by the triplets (a_i,b_i,τ_i) , $i=1,2,\ldots,8$, resulting in 24 variables in total. The number of variables can be reduced when the properties of $u^*(t)$ are considered. The advantage of the parametric approach is that it reduces the optimal control policy to the simple structure above and replaces a complicated analysis by a computationally efficient scheme suitable for real-time implementation.

Let us define

$$J_i^u = \int_{\tau_{i-1}}^{\tau_i} u^2(t)dt$$
 (20)

as the energy cost during the interval $[\tau_{i-1}, \tau_i]$. Problem 1 is now equivalently transformed into a static parametric optimization problem:

Problem 2: TOSTC problem

$$\min \rho_t \tau_8 + \rho_u \sum_{i=1}^8 J_i^u$$

subject to

$$v_{\min} < v\left(\tau_i\right) < v_{\max},\tag{21}$$

$$(a_i \tau_i + b_i) (a_i \tau_{i-1} + b_i) \ge 0,$$
 (22)

$$u_{\min} \le a_i \tau_i + b_i \le u_{\max},\tag{23}$$

$$\tau_{i-1} \le \tau_i, \quad i = 1, \dots, 8, \tag{24}$$

$$u_{\min} \le a_1 \tau_0 + b_1 \le u_{\max},\tag{25}$$

$$\underline{t}_1 \le \tau_5 \le \bar{t}_1,$$
 (26)
 $x(\tau_5) = l_1$ (27)

$$t_2 \le \tau_8 \le \bar{t}_2,\tag{28}$$

$$x\left(\tau_{8}\right) = l_{1} + l_{2} \tag{29}$$

where $J_i^u, v(\tau_i)$ in (21), and $x(\tau_i)$ in (27) and (29) can be expressed as

$$J_i^u = \frac{a_i^2}{3} \left(\tau_i^3 - \tau_{i-1}^3 \right) + a_i b_i \left(\tau_i^2 - \tau_{i-1}^2 \right) + b_i^2 \left(\tau_i - \tau_{i-1} \right)$$

$$v(\tau_i) = v(\tau_{i-1}) + b_i(\tau_i - \tau_{i-1}) + \frac{a_i}{2}(\tau_i^2 - \tau_{i-1}^2)$$

and

$$x(\tau_{i}) = x(\tau_{i-1}) + v(\tau_{i-1})(\tau_{i} - \tau_{i-1}) + \frac{b_{i}}{2}(\tau_{i} - \tau_{i-1})^{2} + \frac{a_{i}}{6}(\tau_{i}^{3} + 2\tau_{i-1}^{3} - 3\tau_{i-1}^{2}\tau_{i})$$

respectively, from Lemma 1.

Remark 3: Problem 2 is equivalent to Problem 1, where the continuous velocity constraint (7) is ensured by (21) and

(22). The continuous acceleration constraints (8) are ensured by (23) and (25). The constraints (24) are needed to ensure the correct order of the critical times defining the linear segments of $u^*(t)$ in (19).

Remark 4: The parametric optimization framework is very general so that it can be used to solve many different trajectory optimization problems. It can also easily incorporate an initial acceleration condition, interior and terminal velocity/acceleration constraints by adding additional equality or inequality constraints.

Remark 5: We can add the jerk constraints $|a_i| \le a_J$ to smooth the acceleration profile, where a_i corresponds to the jerk profile, and a_J is a given limit of jerk tolerance [13].

IV. EXTENSION TO MULTIPLE GATEWAYS

The proposed parametric framework for two gateways can be easily extended to the case of more than two gateways. We can use three triplets (a_i,b_i,τ_i) to parameterize the optimal acceleration profile for a single gateway. For two gateways, eight triplets (a_i,b_i,τ_i) are enough to parameterize the optimal acceleration profile. The following result shows the number of triplets needed for general N gateways.

Lemma 2: A total of 5(N-1)+3 triplets of (a_i,b_i,τ_i) are needed to characterize the optimal acceleration profile for N gateways.

Proof: We prove the result by mathematical induction. For a single and double gateways, 3 and 8 triplets are needed, respectively. Therefore, we can assume that 5(k-1)+3 triplets are needed for k gateways.

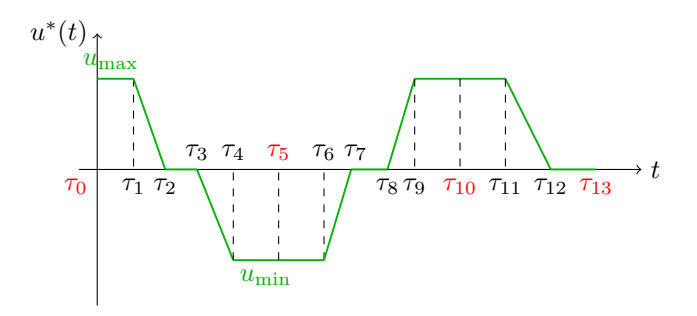


Fig. 4. Optimal acceleration profile for three intersections, where the time instants in red signify the gateway crossing time

For k+1 gateways, the value of $u(\tau_{5k})$ does not need to be zero at gateway k, which corresponds to τ_8 in Fig. 3. When the costate $\lambda_2(\tau_{5k-2})=0$ such as τ_8 in Fig. 4, it can keep decreasing until $u(t)=u_{\max}$, which corresponds to τ_9 in Fig. 4. In this case, the agent arrives at gateway k at τ_{5k} such as τ_{10} in Fig. 4. Then the control input decreases from u_{\max} to 0 from τ_{5k+1} to τ_{5k+2} , for example, τ_{11} to τ_{12} as shown in Fig. 4. Therefore, we can conclude that 5(N-1)+3 triplets are enough to characterize the optimal acceleration profile for N gateways.

Let J_i^u be the energy cost during the interval $[\tau_{i-1}, \tau_i]$ defined in (20). Therefore, for N gateways, the TOSTC problem can be solved by the following optimization problem: Problem 3: TOSTC problem

$$\min \rho_t \tau_{5(N-1)+3} + \rho_u \sum_{i=1}^{5(N-1)+3} J_i^u$$

subject to

$$v_{\min} \le v\left(\tau_i\right) \le v_{\max} \tag{30}$$

$$(a_i \tau_i + b_i) (a_i \tau_{i-1} + b_i) \ge 0$$
 (31)

$$u_{\min} \le a_i \tau_i + b_i \le u_{\max},\tag{32}$$

$$\tau_{i-1} \le \tau_i, i = 1, 2, \dots, 5(N-1) + 3,$$
(33)

$$u_{\min} \le a_1 \tau_0 + b_1 \le u_{\max},\tag{34}$$

$$\underline{t}_{\lceil \frac{j}{\bar{z}} \rceil} \le \tau_j \le \bar{t}_{\lceil \frac{j}{\bar{z}} \rceil},\tag{35}$$

$$x(\tau_j) = \sum_{i=1}^{\left\lceil \frac{j}{5} \right\rceil} l_i \tag{36}$$

$$j = 5, 10, \dots, 5(N-1), 5(N-1) + 3,$$
 (37)

where $\lceil x \rceil$ is the smallest integer greater than or equal to x, J_i^u , $v(\tau_i)$ and $x(\tau_i)$ can be expressed as

$$J_i^u = \frac{a_i^2}{3} \left(\tau_i^3 - \tau_{i-1}^3 \right) + a_i b_i \left(\tau_i^2 - \tau_{i-1}^2 \right) + b_i^2 \left(\tau_i - \tau_{i-1} \right)$$
$$v \left(\tau_i \right) = v \left(\tau_{i-1} \right) + b_i \left(\tau_i - \tau_{i-1} \right) + \frac{a_i}{2} \left(\tau_i^2 - \tau_{i-1}^2 \right)$$

and

$$x(\tau_{i}) = \sum_{j=1}^{i-1} l_{j} + v(\tau_{i-1})(\tau_{i} - \tau_{i-1}) + \frac{b_{i}}{2}(\tau_{i} - \tau_{i-1})^{2} + \frac{a_{i}}{6}(\tau_{i}^{3} + 2\tau_{i-1}^{3} - 3\tau_{i-1}^{2}\tau_{i}),$$

respectively, from Lemma 1.

Remark 6: This remark pertains to the overall complexity of the proposed algorithm. At each gateway i, the gateway open intervals corresponding to $\rho_t=0$ (minimum energy interval) and $\rho_u=0$ (minimum time interval) are calculated. All gateway open intervals between the minimum energy interval and the minimum time interval are considered as feasible intervals. Suppose that there are n_i feasible intervals to cross gateway i. At most, there are $\prod_{i=1}^N n_i$ different paths to cross all gateways. Some of the paths such as $\underline{t}_{i-1} \geq \overline{t}_i$ or when it is impossible to travel a distance l_i using the time $\overline{t}_i - \underline{t}_{i-1}$, could be eliminated by the pruning algorithm. For each possible path, Problem 3 needs to be solved, which involves 15N-6 variables with 32N-10 inequality constraints and 16N-6 equality constraints.

A. Special Case: Single Gateway

Assume that there is only one gateway. We can conclude from Fig. 2 that the control input only contains acceleration or deceleration, not both. Therefore, the optimal acceleration profile can be parameterized as

$$u^*(t) = a_i t + b_i \text{ for } t \in [\tau_{i-1}, \tau_i]$$

for i=1,2,3, where $\tau_0=t_0$, and $\tau_3=t_1$. Here we assume that trip time t_1 belongs to some known interval $[\underline{t}_1,\overline{t}_1]$. Due to physical constraints, there are only a limited number of possibilities for the gateway crossing interval. Let J_i^u be the energy cost during the interval $[\tau_{i-1},\tau_i]$ defined in (20). The optimal parameters (a_i,b_i,τ_i) for i=1,2,3 can be obtained by solving the following optimization problem:

Problem 4: TOSTC problem

$$\min \rho_t \tau_3 + \rho_u \sum_{i=1}^3 J_i^u$$

subject to

$$v_{\min} \le v\left(\tau_3\right) \le v_{\max} \tag{38}$$

$$u_{\min} \le a_1 \tau_0 + b_1 \le u_{\max} \tag{39}$$

$$u_{\min} \le a_i \tau_i + b_i \le u_{\max},\tag{40}$$

$$\tau_{i-1} \le \tau_i, \quad i = 1, \dots, 3 \tag{41}$$

$$t_1 \le \tau_3 \le \bar{t}_1 \tag{42}$$

$$x\left(\tau_3\right) = l,\tag{43}$$

where J_i^u , $x(\tau_i)$, and $v(\tau_i)$ can be expressed as

$$J_{i}^{u} = \frac{a_{i}^{2}}{3} \left(\tau_{i}^{3} - \tau_{i-1}^{3} \right) + a_{i} b_{i} \left(\tau_{i}^{2} - \tau_{i-1}^{2} \right) + b_{i}^{2} \left(\tau_{i} - \tau_{i-1} \right)$$
$$x \left(\tau_{i} \right) = x \left(\tau_{i-1} \right) + v \left(\tau_{i-1} \right) \left(\tau_{i} - \tau_{i-1} \right)$$
$$+ \frac{b_{i}}{2} \left(\tau_{i} - \tau_{i-1} \right)^{2} + \frac{a_{i}}{6} \left(\tau_{i}^{3} + 2 \tau_{i-1}^{3} - 3 \tau_{i-1}^{2} \tau_{i} \right)$$

and

$$v(\tau_i) = v(\tau_{i-1}) + b_i(\tau_i - \tau_{i-1}) + \frac{a_i}{2}(\tau_i^2 - \tau_{i-1}^2)$$

respectively, according to Lemma 1.

Remark 7: Note that we do not include the constraint (31) here since we have established that the optimal acceleration profile contains either acceleration or deceleration, but not both. Therefore, the terminal velocity constraint (38) can replace the velocity constraints (30).

V. APPLICATION TO AUTONOMOUS VEHICLE ECO-DRIVING PROBLEMS

Although vehicle dynamics can be very complicated, it is common practice to use the purely kinematic model in (1) to design a speed profile, and assume that the vehicle power train dynamics are able to track the speed profile obtained from the kinematic model. Vehicles also have physical acceleration/deceleration constraints as in (3). According to traffic laws, on-road vehicles have to travel below the speed limit posted, and the constraint (2) could be different on different roads, such as

$$0 \le \underline{v}_i \le v(t) \le \overline{v}_i \quad \text{for } \sum_{j=1}^{i-1} l_j < x(t) \le \sum_{j=1}^{i} l_j, \qquad (44)$$

where \bar{v}_i and \underline{v}_i are the maximum and minimum speed limits on link i. The operation of a traffic signal is equivalent to the switching behavior of a gateway. When facing green lights, vehicles are free to pass the intersection; while when facing red lights, vehicles must come to a full stop and wait for the traffic signal to turn green. In the ECO-AND problem when $\rho_t=0$, autonomous vehicles can be controlled to travel around the speed limit at a constant speed in an urban environment. The only time that the speed changes is to increase it in order to beat the green signal or to slow down to avoid the red traffic signal. Therefore, the most energy-efficient manner to operate an autonomous vehicle is to avoid unnecessary braking and acceleration. The eco-driving problem of autonomous vehicles

crossing multiple intersections has the same objective as that in (4), where J^u well captures the eco-driving behavior to penalize the acceleration and deceleration.

The previous results show that the optimal solution $u^*(t)$ has a piece-wise linear form u(t) = at + b, which captures most acceleration profiles used in the literature and vehicle simulation software [23]. When a = b = 0, the vehicle travels at a constant speed. When a = 0, the acceleration profile becomes either constant acceleration (b > 0) or constant deceleration (b < 0). When $a \neq 0$, the resulting linear acceleration profile is also called "smooth jerk" [23].

Remark 8: For autonomous vehicle eco-driving problems, some practical issues have to be considered. First, by taking driving comfort into account, we have to add the constraints $|a_i| \leq \bar{a}$, where a_i in the parametric form $u_i = a_i t + b_i$ corresponds to the jerk profile, and \bar{a} is the limit of jerk tolerance. The value \bar{a} is reported to be 10 m/s^3 in [13]. Second, when an autonomous vehicle turns at intersections, the arrival speed should be constrained for purposes of safety and ride comfort, i.e., $v(t_i) \leq v^c$, where v^c is some comfort speed for turning. Finally, when an autonomous vehicle is commanded to approach a traffic light at the exact time that the traffic light changes from red to green, this may provide discomfort to the passengers. Therefore, a safety buffer δ may be added to the start of green lights, i.e. the feasible intersection crossing time is re-defined as $\hat{T}_i^o = \{t | [t - \delta, t] \subseteq t \}$ T_i^o }.

The ECO-AND problem can be formulated as

Problem 5: ECO-AND Problem

$$\min_{u(t)} \rho_t \left(t_N - t_0 \right) + \rho_u \int_{t_0}^{t_N} u^2 \left(t \right) dt$$

subject to (1) and

$$x(t_i) = \sum_{j=1}^{i} l_j, \ i = 1, \dots, N$$
 (45)

$$\underline{v}_i \le v(t) \le \overline{v}_i$$
 for $\sum_{j=1}^{i-1} l_j < x(t) \le \sum_{j=1}^{i} l_j$ (46)

$$u_{\min} \le u(t) \le u_{\max} \tag{47}$$

$$|\dot{u}(t)| \le \bar{a} \tag{48}$$

$$t_i \in \hat{T}_i^o, \ i = 1, \dots, N. \tag{49}$$

Let J_i^u be the energy cost during the interval $[\tau_{i-1}, \tau_i]$ defined in (20). Then, based on the results in Section IV, the ECO-AND problem can be solved by the following optimization problem:

Problem 6: ECO-AND problem

$$\min \rho_t \tau_{5(N-1)+3} + \rho_u \sum_{i=1}^{5(N-1)+3} J_i^u$$

subject to

$$\underline{v}_{\lceil \frac{i}{5} \rceil} \leq v (\tau_i) \leq \overline{v}_{\lceil \frac{i}{5} \rceil}
(a_i \tau_i + b_i) (a_i \tau_{i-1} + b_i) \geq 0
u_{\min} \leq a_i \tau_i + b_i \leq u_{\max},
|a_i| \leq \overline{a},
\tau_{i-1} \leq \tau_i,
i = 1, 2, \dots, 5 (N-1) + 3,
u_{\min} \leq a_1 \tau_0 + b_1 \leq u_{\max},
x (\tau_j) = \sum_{i=1}^{\lceil \frac{i}{5} \rceil} l_i, \tau_j \in \hat{T}_{\lceil \frac{i}{5} \rceil}^o,
j = 5, 10, \dots, 5 (N-1), 5 (N-1) + 3,$$

where $\lceil x \rceil$ is the smallest integer greater than or equal to x, J_i^u , $v(\tau_i)$, and $x(\tau_i)$ can be expressed as

$$J_{i}^{u} = \frac{a_{i}^{2}}{3} \left(\tau_{i}^{3} - \tau_{i-1}^{3} \right) + a_{i} b_{i} \left(\tau_{i}^{2} - \tau_{i-1}^{2} \right) + b_{i}^{2} \left(\tau_{i} - \tau_{i-1} \right)$$
$$v \left(\tau_{i} \right) = v \left(\tau_{i-1} \right) + b_{i} \left(\tau_{i} - \tau_{i-1} \right) + \frac{a_{i}}{2} \left(\tau_{i}^{2} - \tau_{i-1}^{2} \right)$$

and

$$x(\tau_i) = \sum_{j=1}^{i-1} l_j + v(\tau_{i-1})(\tau_i - \tau_{i-1}) + \frac{b_i}{2}(\tau_i - \tau_{i-1})^2 + \frac{a_i}{6}(\tau_i^3 + 2\tau_{i-1}^3 - 3\tau_{i-1}^2\tau_i)$$

respectively, from Lemma 1.

A. ECO-AND Problem For An Isolated Signalized Intersection

Based on our analysis for a single intersection [20], the optimal acceleration profile can be parameterized as

$$u^*(t) = a_i t + b_i \text{ for } t \in [\tau_{i-1}, \tau_i]$$

for i=1,2,3, where $\tau_0=t_0$, and $\tau_3=t_1$. Let J_i^u be the energy cost during the interval $[\tau_{i-1},\tau_i]$ defined in (20). The optimal parameters (a_i,b_i,τ_i) for i=1,2,3 can be obtained by solving the following optimization problem:

Problem 7: ECO-AND problem

$$\min \rho_t \tau_3 + \rho_u \sum_{i=1}^3 J_i^u$$

subject to

$$v_{\min} < v\left(\tau_3\right) < v_{\max} \tag{50}$$

$$u_{\min} \le a_1 \tau_0 + b_1 \le u_{\max} \tag{51}$$

$$u_{\min} \le a_i \tau_i + b_i \le u_{\max},\tag{52}$$

$$|a_i| \le \bar{a} \tag{53}$$

$$\tau_{i-1} \le \tau_i, \quad i = 1, \dots, 3 \tag{54}$$

$$x\left(\tau_{3}\right) = l, \tau_{3} \in \hat{T}_{1}^{o} \tag{55}$$

where J_{i}^{u} , $v\left(\tau_{i}\right)$, and $x\left(\tau_{i}\right)$ can be expressed as

$$J_i^u = \frac{a_i^2}{3} \left(\tau_i^3 - \tau_{i-1}^3 \right) + a_i b_i \left(\tau_i^2 - \tau_{i-1}^2 \right) + b_i^2 \left(\tau_i - \tau_{i-1} \right)$$
$$v \left(\tau_i \right) = v \left(\tau_{i-1} \right) + b_i \left(\tau_i - \tau_{i-1} \right) + \frac{a_i}{2} \left(\tau_i^2 - \tau_{i-1}^2 \right)$$

TABLE I

OPTIMAL PERFORMANCE FOR DIFFERENT WEIGHT PARAMETERS

$ ho_t$	$ ho_u$	t_1	t_2	J^t	J^u	J
0	1	0.9437	4.2294	7.0000	0.2330	0.2330
0.25	0.75	0.9276	4.1020	6.8527	0.2761	1.9203
1	0	0.9205	4.0000	6.7312	0.3217	6.7311

and

$$x(\tau_{i}) = x(\tau_{i-1}) + v(\tau_{i-1})(\tau_{i} - \tau_{i-1}) + \frac{b_{i}}{2}(\tau_{i} - \tau_{i-1})^{2} + \frac{a_{i}}{6}(\tau_{i}^{3} + 2\tau_{i-1}^{3} - 3\tau_{i-1}^{2}\tau_{i})$$

respectively, according to Lemma 1.

In the above solution, we do not consider the case of turning. When a vehicle makes a turn in an intersection, this intersection may be signalized or not. For signalized intersections, we can just add the constraint $v(\tau_j) \leq v^c$ when vehicles make a turn at $x(\tau_j)$. When vehicles make a turn at non-signalized intersections, we can treat the intersection as a signalized intersection but with $\hat{T}_i^o = [0, \infty)$.

VI. SIMULATION EXAMPLES

We evaluate the proposed solution by testing the following scenario with three gateways, where Problem 3 is solved by the fmincon function in the Optimization Toolbox in MATLAB. The lengths between any two consecutive gateways are generated randomly by uniformly distributed numbers between 1 and 10. In our case, the lengths are 1.0934 m, $5.5169 \, m$ and $5.4620 \, m$, which correspond to the gaps between horizontal lines in Fig. 5. Each alternates between open and closed states with a period of time 1 second. The initial speed is $v_0 = 1 m/s$, and the maximum speed is set as $v_{\rm max}=2~m/s$. The maximum acceleration and deceleration are $u_{\rm max}=1~m/s^2$ and $u_{\rm min}=-1~m/s^2$. It is not difficult to figure out that the agent should cross the first gateway in the interval [0, 1] due to the acceleration and speed constraints. Since the maximum speed of the agent is 2 m/s, it is not possible for agents to cross the second gateway during [2,3]when it is open. Therefore, the agent should pass the second gateway in the interval [4,5]. Finally, the agent should pass the third gateway in the interval [6, 7]. Once all the feasible intervals are determined, we can solve the TOSTC Problem 3. Let us consider three different cases: case 1 ($\rho_t = 0$ and $\rho_u=1$), case 2 ($\rho_t=0.25$ and $\rho_u=0.75$), and case 3 $(\rho_t = 1 \text{ and } \rho_u = 0)$. The optimal speed, acceleration and distance profiles are depicted in Fig. 5 for these three different cases. The gateway crossing times, the energy cost, and the total cost are shown in Table I. The first case responds to the energy optimal solution. In this case, the agent chooses to pass the third gateway at the latest feasible time within the interval [6, 7]. The third case corresponds to the time-optimal solution. In this case, the agent reaches the maximum speed exactly at the second gateway, which is the earliest feasible time.

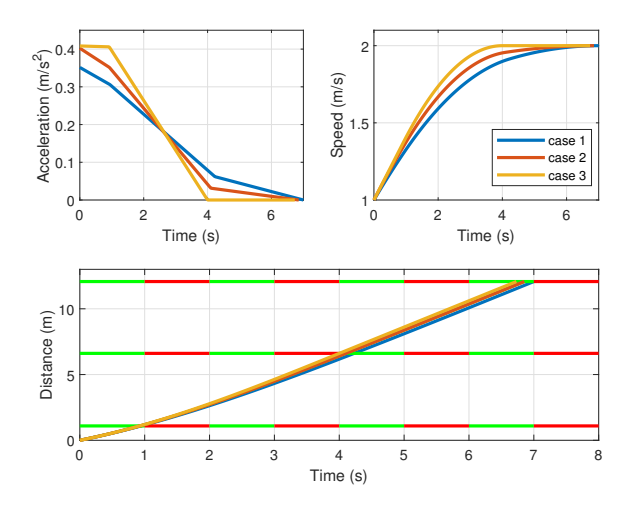


Fig. 5. Optimal acceleration, speed and distance profiles for the cases in Table I.

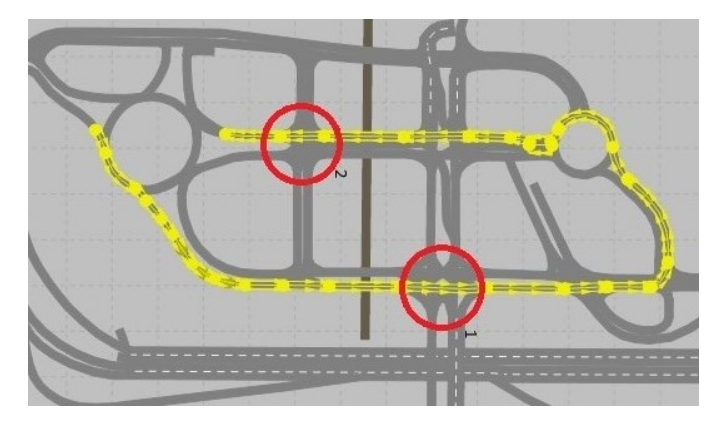


Fig. 6. Mcity test route

A. ECO-AND Problem for Multiple Signalized Intersections

We evaluate the proposed solution by testing the following scenario with two intersections in Mcity - an automated and connected car test facility in Ann Arbor, Michigan, where the test route with two signalized intersections circled is shown in Fig. 6. Two phases were set up for each traffic signal for simplicity. The cycle time for the first traffic signal is 76 seconds, where the green time is 34 seconds and the red time is 42 seconds. The cycle time for the second traffic signal is 32 seconds, where the green time is 12 seconds and the red time is 20 seconds. The distance between the two traffic lights is 312 meters. Autonomous vehicles receive phase and time information of both traffic lights with a distance of 150 meters to the first traffic light, and the speed is $11.25 \ m/s$. Currently, both traffic lights are red. The times until the next green are 17 seconds and 7 seconds, for the first and second traffic signals, respectively. The speed limits are set as $v_{\min} =$ 2.78~m/s, and $v_{\rm max}=20~m/s$. The maximum acceleration and deceleration are $u_{\text{max}} = 2.5 \text{ m/s}^2$ and $u_{\text{min}} = -2.9$ m/s^2 . Here we choose $\rho_t = 0.0036$ and $\rho_u = 0.0093$, where their values are calculated based on the normalization procedure in [20] with $\rho = 0.6$. The parameter $\rho \in [0, 1]$

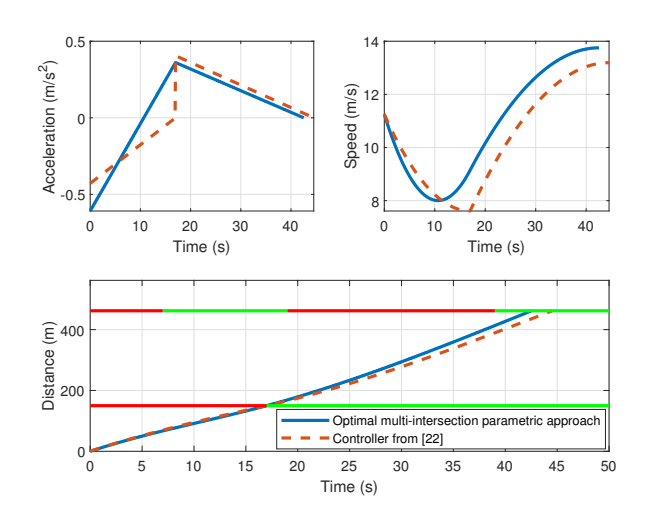


Fig. 7. Distance profile of different methods.

in [20] captures the trade-off between minimizing the travel time $(\rho = 1)$ and minimizing the energy consumption $(\rho =$ 0). We use our previous approach for a single intersection [20] as the baseline scenario, which solves the eco-driving problem for each road segment individually, and compare the proposed solution and the baseline scenario. Even though our previous approach [20] calculates the optimal performance for each road segment, it is not the optimal solution for the combined two segments as a whole. Overall, the optimal multiintersection parametric approach outperforms [20] by 3.13%. Figure 7 shows the acceleration, speed, and distance profiles for both the optimal multi-intersection parametric approach (blue solid curve) and [20] (orange dashed curve). In addition, the speed profile of the optimal multi-intersection parametric approach is smoother than that of [20] as seen from Fig. 7. We can see from Fig. 7 that the intersection crossing times of both approaches are within the green light interval. The travel times are 42.5407 and 44.5333 seconds for the optimal multiintersection parametric approach and [20], respectively. Also note that all speed and acceleration constraints are satisfied for both approaches.

VII. CONCLUSIONS

A thorough analysis is presented to identify the optimal acceleration profile for a class of trajectory optimization problems with spatio-temporal constraints. A parametrization method is used to transform the dynamic trajectory optimization into a static parameter optimization. The proposed framework is applied to solve the eco-driving problem of autonomous vehicles approaching multiple signalized intersections. The effectiveness of the proposed method is demonstrated by simulation results. The results here are limited to autonomous vehicles in the free flow mode, and the case with interfering traffic is studied in [24].

REFERENCES

 J. Cortes, S. Martinez, T. Karatas, and F. Bullo, "Coverage control for mobile sensing networks," *IEEE Trans. Robot. Automat.*, vol. 20, no. 2, pp. 243–255, 2004.

- [2] Y. Kantaros, M. Thanou, and A. Tzes, "Distributed coverage control for concave areas by a heterogeneous robot swarm with visibility sensing constraints," *Automatica*, vol. 53, pp. 195 – 207, 2015.
- [3] X. Meng, A. Houshmand, and C. G. Cassandras, "Multi-agent coverage control with energy depletion and repletion," in *Proc. of IEEE 57th Conf.* on *Decision and Control*, 2018, pp. 2101–2106.
- [4] G. Mahler and A. Vahidi, "An optimal velocity-planning scheme for vehicle energy efficiency through probabilistic prediction of traffic-signal timing," *IEEE Trans. Intell. Transport. Syst.*, vol. 15, no. 6, pp. 2516– 2523, 2014.
- [5] A. Ferrara, S. Sacone, and S. Siri, Freeway Traffic Modelling and Control, ser. Advances in Industrial Control. Springer, 2018.
- [6] Y. Khazaeni and C. G. Cassandras, "Event-driven trajectory optimization for data harvesting in multi-agent systems," *IEEE Trans. Control Netw.* Syst., 2017.
- [7] N. Nigam, S. Bieniawski, I. Kroo, and J. Vian, "Control of multiple uavs for persistent surveillance: Algorithm and flight test results," *IEEE Trans. Control Syst. Technol.*, vol. 20, no. 5, pp. 1236–1251, 2012.
- [8] C. G. Cassandras, X. Lin, and X. Ding, "An optimal control approach to the multi-agent persistent monitoring problem," *IEEE Trans. Autom. Control*, vol. 58, no. 4, pp. 947–961, 2013.
- [9] Z. Tang and U. Ozguner, "Motion planning for multitarget surveillance with mobile sensor agents," *IEEE Transactions on Robotics*, vol. 21, no. 5, pp. 898–908, 2005.
- [10] K. Leahy, D. Zhou, C.-I. Vasile, K. Oikonomopoulos, M. Schwager, and C. Belta, "Persistent surveillance for unmanned aerial vehicles subject to charging and temporal logic constraints," *Autonomous Robots*, vol. 40, no. 8, pp. 1363–1378, 2016.
- [11] X. Ding, S. L. Smith, C. Belta, and D. Rus, "Optimal control of markov decision processes with linear temporal logic constraints," *IEEE Trans. Autom. Control*, vol. 59, no. 5, pp. 1244–1257, 2014.
- [12] C. Baier and J.-P. Katoen, Principles of model checking. MIT press, 2008.
- [13] M. Barth, S. Mandava, K. Boriboonsomsin, and H. Xia, "Dynamic ecodriving for arterial corridors," in *Proc. IEEE Forum on Integrated and Sustainable Transportation Systems*, 2011, pp. 182–188.
- [14] B. Asadi and A. Vahidi, "Predictive cruise control: Utilizing upcoming traffic signal information for improving fuel economy and reducing trip time," *IEEE Trans. Control Syst. Technol.*, vol. 19, no. 3, pp. 707–714, 2011.
- [15] E. Ozatay, U. Ozguner, D. Filev, and J. Michelini, "Analytical and numerical solutions for energy minimization of road vehicles with the existence of multiple traffic lights," in *Proc. 52nd IEEE Conf. Decision Control*, 2013, pp. 7137–7142.
- [16] M. Corno, A. Bisoffi, C. Ongini, and S. M. Savaresi, "An energy-driven road-to-driver assistance system for intersections," in *Proc. European Control Conf.*, 2015, pp. 3035–3040.
- [17] N. Wan, A. Vahidi, and A. Luckow, "Optimal speed advisory for connected vehicles in arterial roads and the impact on mixed traffic," *Transport. Res. Part C: Emerg. Technol.*, vol. 69, pp. 548 – 563, 2016.
- [18] G. De Nunzio, C. Canudas de Wit, P. Moulin, and D. Di Domenico, "Eco-driving in urban traffic networks using traffic signals information," *Int. J. Robust & Nonlinear Control*, vol. 26, no. 6, pp. 1307–1324, 2016.
- [19] X. Huang and H. Peng, "Speed trajectory planning at signalized intersections using sequential convex optimization," in *Proc. American Control Conf.*, 2017, pp. 2992–2997.
- [20] X. Meng and C. G. Cassandras, "Optimal control of autonomous vehicles for non-stop signalized intersection crossing," in *Proc. of the* 57th IEEE Conf. on Decision and Control, 2018, pp. 6988–6993.
- [21] R. F. Hartl, S. P. Sethi, and R. G. Vickson, "A survey of the maximum principles for optimal control problems with state constraints," *SIAM Review*, vol. 37, no. 2, pp. 181–218, 1995.
- [22] A. E. Bryson and Y. C. Ho, Applied optimal control: optimization, estimation and control. Taylor & Francis, 1975.
- [23] *PreScan*, Version 7.6.0 ed., TASS International, https://tass.plm.automation.siemens.com/prescan.
- [24] X. Meng and C. G. Cassandras, "A real-time optimal eco-driving approach for autonomous vehicles crossing multiple signalized intersections," in 2019 American Control Conference (ACC), 2019, pp. 3593– 3598.



XIANGYU MENG was born in Changchun, Jilin, CHINA. He received the B.S. degree in information and computing science from Harbin Engineering University, and M.S. degree in control science and engineering from Harbin Institute of Technology, Harbin, CHINA, in 2006 and 2008, respectively. He received the Ph.D. degree in electrical and computer engineering from the University of Alberta, Edmonton, Alberta, CANADA, in 2014.

From June 2007 to July 2007, and from November 2007 to January 2008, he was a Research Associate with the Department of Mechanical Engineering, University of Hong Kong. From February 2009 to August 2010, he was a Research Award Recipient in the Department of Electrical and Computer Engineering, University of Alberta. From December 2014 to December 2016, he was a Research Fellow with the School of Electrical and Electronic Engineering, Nanyang Technological University, Singapore. From January 2017 to December 2018, he was a Postdoctoral Associate with the Division of Systems Engineering, Boston University, USA. Since 2019, he has been an Assistant Professor with the Division of Electrical and Computer Engineering, Louisiana State University, Baton Rouge, LA, USA. His research interests include connected and autonomous vehicles, multiagent networks, and cyber-physical systems.



Christos G. Cassandras (F'96) is Distinguished Professor of Engineering at Boston University. He is Head of the Division of Systems Engineering, Professor of Electrical and Computer Engineering, and co-founder of Boston University's Center for Information and Systems Engineering (CISE). He received degrees from Yale University, Stanford University, and Harvard University. In 1982–84 he was with ITP Boston, Inc. where he worked on the design of automated manufacturing systems. In 1984–1996 he was a

faculty member at the Department of Electrical and Computer Engineering, University of Massachusetts/Amherst. He specializes in the areas of discrete event and hybrid systems, cooperative control, stochastic optimization, and computer simulation, with applications to computer and sensor networks, manufacturing systems, and transportation systems. He has published over 400 refereed papers in these areas, and six books. He has guest-edited several technical journal issues and currently serves on several journal Editorial Boards, including Editor of Automatica. In addition to his academic activities, he has worked extensively with industrial organizations on various systems integration projects and the development of decision support software. He has most recently collaborated with The MathWorks, Inc. in the development of the discrete event and hybrid system simulator SimEvents. Dr. Cassandras was Editor-in-Chief of the IEEE Transactions on Automatic Control from 1998 through 2009 and has also served as Editor for Technical Notes and Correspondence and Associate Editor. He was the 2012 President of the IEEE Control Systems Society (CSS). He has also served as Vice President for Publications and on the Board of Governors of the CSS, as well as on several IEEE committees, and has chaired several conferences. He has been a plenary/keynote speaker at numerous international conferences, including the 2017 IFAC World Congress, the American Control Conference in 2001 and the IEEE Conference on Decision and Control in 2002 and 2016, and has also been an IEEE Distinguished Lecturer. He is the recipient of several awards, including the 2011 IEEE Control Systems Technology Award, the Distinguished Member Award of the IEEE Control Systems Society (2006), the 1999 Harold Chestnut Prize (IFAC Best Control Engineering Textbook) for Discrete Event Systems: Modeling and Performance Analysis, a 2011 prize and a 2014 prize for the IBM/IEEE Smarter Planet Challenge competition, the 2014 Engineering Distinguished Scholar Award at Boston University, several honorary professorships, a 1991 Lilly Fellowship and a 2012 Kern Fellowship. He is a member of Phi Beta Kappa and Tau Beta Pi. He is also a Fellow of the IEEE and a Fellow of the IFAC.